I&EC research
Industrial & Engineering Chemistry Research

Article

pubs.acs.org/IECR

Evaluation of the Conductor-like Screening Model for Real Solvents for the Prediction of the Water Activity Coefficient at Infinite Dilution in Ionic Liquids

Kiki A. Kurnia,[†] Simão P. Pinho,[‡,§] and João A. P. Coutinho*[,†]

[†]Departamento de Química, CICECO, Universidade de Aveiro, 3810-193 Aveiro, Portugal
[‡]Associate Laboratory LSRE/LCM, Instituto Politécnico de Bragança, 5301-857 Bragança, Portugal
[§]UNIFACS-Universidade de Salvador, 41770-235 Salvador, Brazil

Supporting Information

ABSTRACT: Ionic liquids (ILs) have attracted great attention, from both industry and academia, as alternative fluids for very different types of applications. The large number of cations and anions allow a wide range of physical and chemical characteristics to be designed. However, the exhaustive measurement of all these systems is impractical, thus requiring the use of a predictive model for their study. In this work, the predictive capability of the conductor-like screening model for real solvents (COSMO-RS), a model based on unimolecular quantum chemistry calculations, was evaluated for the prediction water activity coefficient at infinite dilution, γ_w^∞, in several classes of ILs. A critical evaluation of the experimental and predicted data using COSMO-RS was carried out. The global average relative deviation was found to be 27.2%, indicating that the model presents a satisfactory prediction ability to estimate γ_w^∞ in a broad range of ILs. The results also showed that the basicity of the ILs anions plays an important role in their interaction with water, and it considerably determines the enthalpic behavior of the binary mixtures composed by ILs and water. Concerning the cation effect, it is possible to state that generally γ_w^∞ increases with the cation size, but it is shown that the cation−anion interaction strength is also important and is strongly correlated to the anion ability to interact with water. The results here reported are relevant in the understanding of ILs−water interactions and the impact of the various structural features of ILs on the γ_w^∞ as these allow the development of guidelines for the choice of the most suitable ILs with enhanced interaction with water.

1. INTRODUCTION

Ionic liquids (ILs) are salts with a low melting point and are composed by bulky organic cations coupled with organic or inorganic anions.[1] The most common ILs are based on imidazolium, pyridinium, quaternary ammonium, or quaternary phosphonium cations, but there is a growing interest in many other classes of salts. Since the pioneering work by Walden in 1914,[2] thousands of ILs with unique structures and properties have been reported.[3] An important feature of ILs is that their physical properties, such as density, viscosity, and surface tension, can be manipulated by properly combining the cation and anion to meet the requirement of specific applications, being so referred to as "designer" solvents. Among several industrial applications foreseen, substantial interest has been devoted in the potential of hydrophilic ILs as, to name a few, drying agent,[4] to break the azeotrope in water−alcohol systems,[5−7] and as absorbent in the absorption−refrigeration (AR) systems.[8−11] Among the heat and mass transfer characteristics that should be pursued for more efficient AR applications, criteria to select a suitable absorbent/refrigerant pair requires contributions from thermodynamics. Besides the solubility issues that must be taken into account, high exothermic dilution and strong negative deviation to ideality are desirable, these being the last possible to quantify calculating the water activity coefficient at infinite dilution.[11,12] In this way, the lower the γ^∞ is, the higher is the ILs−water interaction in the system, and vice versa. On the basis of this criterion, mixtures with γ_w^∞ lower than unity present good absorption capacity and are often associated with exothermic mixing behavior.[12] Thus, the water activity coefficient at infinite dilution in IL, γ_w^∞, plays a crucial role on designing and selecting ILs with enhanced interaction with water molecules.

Rationalization of the design of ILs with desirable properties is one of the most fundamental challenges in IL science. Furthermore, with the introduction of the large number of new ILs as potential absorbent, the problem of fast and efficient evaluation of their usefulness in this particular application emerges. This can be done either using time-consuming traditional laboratorial methods, using novel high-throughput experimental methods, or by combining experimental measurements with an initial prescreening by a predictive model, or computational tools. The latter option has proven to be a powerful tool taking into account the rapidly growing number of ILs that makes an experimental screening unfeasible.[13] Many attempts have been made to model and predict the properties of ILs based on group contribution method, regular solution theory, quantitative structure property relationship (QSPR) method,[14−16] and conductor-like screening model for real solvents (COSMO-RS) method.[14,17] At this point, the

Received: May 26, 2014
Revised: July 17, 2014
Accepted: July 17, 2014
Published: July 17, 2014

COSMO-RS model developed by Klamt and co-worker is regarded as a valuable method for predicting the thermodynamic properties of pure ILs or in mixtures, providing an unique a priori computational tool for designing ILs with specific properties.[18,19] This is because the COSMO-RS does not require experimental data, it only requires the structure of the compounds, and therefore, it is applicable to virtually all possible ILs and water mixtures. It should be highlighted that COSMO-RS has already been used to predict γ^{∞} of organic compounds[17,20] and water[21] in ILs. The results suggested that COSMO-RS is capable of giving a priori predictions of the thermodynamics of ionic liquids, which may be of considerable value for the exploration of suitable ILs for practical applications.[17,20,21]

As part of our work on designing ILs for many applications, in the context of this work the aim is to evaluate the capabilities of COSMO-RS to predict water activity coefficient at infinite dilution. For this purpose, a systematic theoretical analysis of ILs−water thermodynamics and energetic interactions was carried out applying the COSMO-RS model, which involved the following steps: (i) evaluating the capability of COSMO-RS to predict the γ_w^{∞}, comparing to the available experimental values in different classes of ILs, (ii) analyzing the relationship between the γ_w^{∞} and the water partial molar excess properties to rationalize and compare the affinity of ILs toward water molecules, and at last (iii) providing a general evaluation of the ILs structure impact toward γ_w^{∞}, so as to provide guidelines to fine-tune ILs with enhanced interaction with water.

2. COSMO-RS

COSMO-RS[15,16] is a well-established method proposed for the prediction of thermophysical properties of fluids based on unimolecular quantum calculations, being an alternative to the structure-interpolating group-contribution methods. The detail theory of COSMO-RS can be found at the original work of Klamt and co-worker.[18,19]

The prediction of γ_w^{∞} in the ILs using COSMO-RS consists of two steps. In the first step, the distinct COSMO files were generated for cations and anions using BP functional B88-p86 with a triple-ξ valence polarized basis set (TZVP) and the resolution of identity standard (RI) approximation using TURBOMOLE 6.1 program package.[22] The subsequent calculations consist mainly of statistical thermodynamics and were performed using COSMOtherm. The parametrization BP_TZVP_C30_1301 (COSMOlogic GmbH & Co KG. Leverkusen, Germany),[23] which is required for the calculation of physiochemical data and contains intrinsic parameters of COSMOtherm and element specific parameters, was adopted.

The activity coefficient of component i is related to its chemical potential μ_i by

$$\gamma_i = \exp\left(\frac{\mu_i - \mu_i^0}{RT}\right) \quad (1)$$

where μ_i^0 is the chemical potential of the pure compound i, R is the ideal gas constant and T the absolute temperature. The detail of the COSMO-RS calculation on determining the chemical potential is given in the COSMO*therm* User's Manual.[23]

In all calculations, ILs were always treated as an equimolar mixture of cation and anion,[24] allowing the study of specific contribution of each counterion. As consequence, predicted γ_w^{∞} values have to be scaled by a factor of 0.5.[17] In addition, the best predictions were obtained with the lowest energy conformations or with the global minimum for both cation and anion.[25] Thus, in this work, the lowest energy conformations of all the species involved were used in the COSMO-RS calculations.

3. RESULT AND DISCUSSIONS

With the aim of understanding ILs−water interaction, the knowledge of water behavior in the pure state as well as in mixtures with ILs is fundamental prerequisite information. Therefore, the discussion of the results begins by describing the molecular behavior of water and the type of molecular interactions occurring in the system using COSMO-RS σ-profiles and σ-potentials. This section is then followed by the validation of the COSMO-RS prediction against experimental data reported in the literature so as to evaluate the molecular interaction between water and ILs with the purpose of finding the key factors governing their interaction.

3.1. σ-Profile and σ-Potential of Water. Among many advantages offered by COSMO-RS,[18] it allows to study the behavior of a molecule in both its pure and mixture states. In this way, COSMO-RS model calculates the thermodynamic properties of compound(s) by using the 3D molecular surface polarity distributions resulting from quantum chemical calculations, and the data is easily visualized in the histogram function called σ-profile and σ-potential.[18] For example, Figure 1 presents the σ-profile and σ-potential for the studied solute,

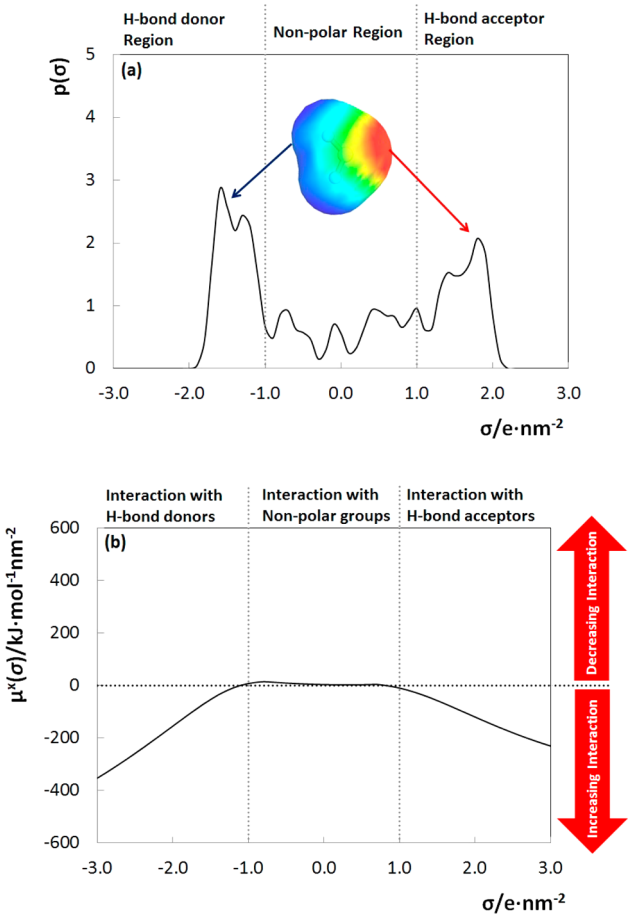

Figure 1. σ-Profile (a) and σ-potential (b) of H_2O computed by COSMO-RS.

dx.doi.org/10.1021/ie5021415 | *Ind. Eng. Chem. Res.* 2014, 53, 12466−12475

H_2O. In general, the COSMO-RS histogram is qualitatively divided into three main regions upon the following cutoff values: hydrogen bond donor ($\sigma < -1$ e·nm^{-2}), nonpolar region ($-1 < \sigma < 1$ e·nm^{-2}), and hydrogen bond acceptor ($\sigma > 1$ e·nm^{-2}). The σ-profile of water (cf. Figure 1a) presents a series of peaks within those three regions, with strong peaks in both the positive and negative polar regions. The high polarized charge at 1.8 e·nm^{-2} corresponds to the oxygen atom fragment (red colored polar surface of the H_2O in Figure 1a), indicating its ability to act as a strong hydrogen-bond acceptor. As consequence, H_2O is attracted to the hydrogen-bond donor, as seen from the σ-potential (cf. Figure 1b). On the other hand, the hydrogen atoms fragment presents a peak within the negative region at -1.6 e·nm^{-2} (blue colored polar surface of the H_2O in Figure 1a) specifying its ability to act as a strong hydrogen-bond donor, and consequently showing attraction toward the hydrogen-bond acceptor, as displayed in the σ-potential. This reflects the amphoteric character of the water molecule, with an excellent ability to act both as a donor and an acceptor for hydrogen bonding.[13] This can be used as input to design potential ILs with high affinity toward water molecules. In this way, it is necessary to design ILs that can act as either hydrogen-bond donor or acceptor. However, it can be appreciated that conventional ILs behave mostly as hydrogen-bond acceptors,[26] hence as will be shown later, the basicity of ILs plays a major role, and the design must focus on how to create ILs with high affinity toward water molecules.

In addition, a series of small peaks within the nonpolar region leads to a decreasing interaction of water molecules toward nonpolar fragments of the other compound in the mixture. Therefore, for example, increasing the alkyl chain of ILs increases its nonpolar character, and it leads to a decreasing affinity of water molecules toward them.

3.2. COSMO-RS Benchmarking: Activity Coefficient at Infinite Dilution. With an aim to evaluate the predictive capability of COSMO-RS, the predicted γ_w^∞ values were compared with experimental data collected from open literature up to February 2014. The name and abbreviation of the ions composing the ILs, for which data are available, are presented in the Supporting Information, Table 1S. To this date, up to 280 experimental data points were found for 53 ILs as listed in Table 2S in the Supporting Information. To assess the performance of COSMO-RS to predict the γ_w^∞, the average relative deviation (ARD) between the experimental and predicted data was determined according to eq 2,

$$\mathrm{ARD}\ (\%) = \frac{1}{N}\sum \left| \frac{\gamma^\infty_{w,\mathrm{COSMO\text{-}RS}} - \gamma^\infty_{w,\mathrm{exp}}}{\gamma^\infty_{w,\mathrm{COSMO\text{-}RS}}} \right| 100 \qquad (2)$$

where $\gamma^\infty_{w,\mathrm{exp}}$ and $\gamma^\infty_{w,\mathrm{COSMO\text{-}RS}}$ are the experimental and predicted water activity coefficients at infinite dilution in ILs, respectively, and N is the number of available data. The $\gamma^\infty_{w,\mathrm{COSMO\text{-}RS}}$ along with the ARD for the studied systems is also given in Table 1S in the Supporting Information. The global ARD of 27.2% indicates that COSMO-RS can predict very satisfactorily the water activity coefficient at infinite dilution in a large variety of ILs. For the system close to ideality, COSMO-RS is able to predict the γ_w^∞ close to the experimental value. For example, COSMO-RS predicts very well the γ_w^∞ in $[NTf_2]$-based ILs as well as its positive deviation from ideality. Furthermore, COSMO-RS can predict the liquid–liquid equilibrium of a system composed of water and $[NTf_2]$-based ILs.[27,28] Nevertheless, it is also worth mentioning that, as depicted in Figure 2,

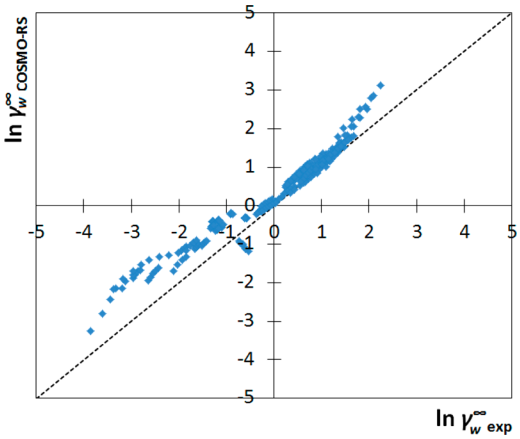

Figure 2. Comparison between experimental and predicted γ_w^∞ using COSMO-RS.

a higher ARD between experimental and predicted values is observed for ILs–water systems with extreme positive (such as [eFAP]-based IL) or negative (regularly observed for ILs containing the $[DMP]^-$, $[TOS]^-$, or especially $[SCN]^-$ anion) deviation from ideality. This observation can be addressed as either (i) the inability of COSMO-RS to correctly predict the γ_w^∞ in very hydrophilic or hydrophobic ILs, thus giving COSMO a room for improvement, or (ii) merely a result of experimental inaccuracy that will be discussed further later.

The large number of the systems available makes a comprehensive study of the influence of the structural characteristic of the ILs on the γ_w^∞ possible, allowing us to draw some heuristics for designing ILs with enhanced interaction with water molecules, for example as absorbent in the absorption–refrigeration systems.[29] The influence of temperature and structural factors, such as cation alkyl chain length, cation head, or functional group and anion nature, are analyzed and discussed regarding their impact on γ_w^∞.

3.2.1. Effect of Temperature. Typical trends describing the temperature dependence of water activity coefficient at infinite dilution in ILs are displayed in Figure 3. The figure presents the experimental data for three different ILs and the predictions using COSMO-RS, displaying different behaviors for the γ_w^∞ temperature dependence. A first type is identified for systems

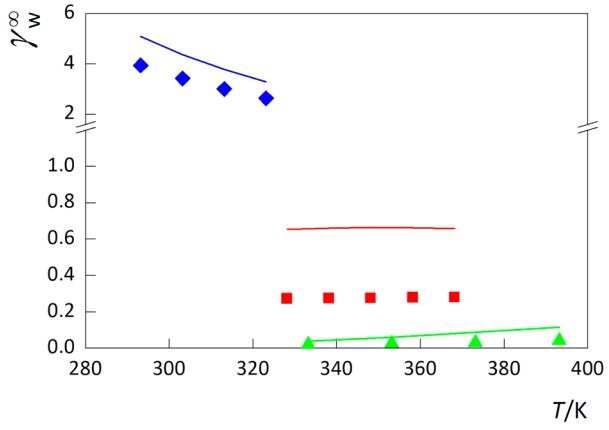

Figure 3. Water infinite dilution activity coefficient in ILs as a function of temperature. Symbols: (blue diamond, line), $[C_4C_1im][NTf_2]$;[39] (red square, line) $[C_4C_1im][SCN]$,[40] and (green triangle, line) $[C_4C_1im][Ac]$.[21]

dx.doi.org/10.1021/ie5021415 | Ind. Eng. Chem. Res. 2014, 53, 12466–12475

presenting water infinite dilution activity coefficients higher than unity (blue colored symbol and line), where their decrease is observed when temperature is increased. In the second type, γ_w^∞ slightly increases, and then decreases with increasing temperature (red colored symbol and line). Finally, the third trend represents systems for which γ_w^∞ increases with temperature (green colored symbol and line). Worth noticing, the last two types of temperature dependence are observed for systems with γ_w^∞ lower than unity, playing a major role in the interactions with water molecules, as will be discussed later. The COSMO-RS predictions capture exactly the same trends for the change of γ_w^∞ with temperature. Additionally, the prediction shows a fair quantitative agreement with the experimental data. The temperature dependence of γ_w^∞ was correlated using eq 3,

$$\ln \gamma_w^\infty = \frac{a}{T} + b \tag{3}$$

The coefficients a and b along with the determination coefficients R^2 are given in the Supporting Information Table 3. As shown in Figure 3, and others throughout this work, the temperature interval is not uniform among the studied ILs. Thus, we used reference temperature, T_{ref}, at 298.15 K to further discuss and analyze the results. The estimated water activity coefficient at infinite dilution from experimental data at reference temperature, T_{ref} = 298.15 K, calculated with these coefficients are given in the Supporting Information Table 3.

The features observed on the $\gamma_w^\infty - T$ diagrams are encouraging toward the use of these predictions for the design of ILs, since they allow us to determine the thermodynamic functions, namely water partial excess Gibbs free energy, $\bar{G}_m^{E,\infty}$; water partial molar excess enthalpy, $\bar{H}_m^{E,\infty}$; and water partial molar excess entropy, $\bar{S}_m^{E,\infty}$, that will help to explore the different trends observed, aiming to find new knowledge for the design of ILs with enhanced interaction with water molecule. Those thermodynamic functions are associated with the changes that occur when water molecules are transferred to a hypothetical diluted ideal solution where the mole fraction of the solvent, in this case the ILs, is equal to 1 and/or the solute is at infinite dilution. Since the experimental activity coefficients of water in ILs were measured at the infinite dilution, the partial molar excess properties were then estimated using the following equations,

$$\bar{G}_m^{E,\infty} = RT \ln(\gamma_w^\infty) \tag{4}$$

$$\bar{H}_m^{E,\infty} = R\left(\frac{\partial \ln \gamma_w^\infty}{\partial \ln(1/T)}\right)_{p,x} \tag{5}$$

$$\bar{S}_m^{E,\infty} = \frac{\bar{H}_m^{E,\infty} - \bar{G}_m^{E,\infty}}{T} \tag{6}$$

where subscripts p and x indicate isobaric condition and constant composition, respectively. The water excess partial molar enthalpy, entropy, and Gibbs energy estimated from experimental data at T_{ref} = 298.15 K are also given in the Supporting Information Table 3.

The estimated water excess partial molar enthalpy, entropy, and Gibbs energy from COSMO-RS, are given in Table 3 in the Supporting Information, displaying the same tendencies as those estimated from the experimental data. The advantage of using COSMO-RS is that the estimated water partial molar excess enthalpy of each species is, within its framework, obtained as the sum of specific interactions, namely electrostatic/misfit, hydrogen bonding, and van der Waals forces.

As observed in Supporting Information Table 3, the dissolution of water molecules to the IL phase is enthalpy driven. This finding is opposite to the dissolution of hydrophobic IL molecules in water, which is driven by entropy.[27,28,30] Exploring the excess properties of the system displayed in Figure 3, it can be observed that the $[C_4C_1im]$-$[NTf_2]$−water system (γ_w^∞ higher than 1) displays a high and positive enthalpy contribution. COSMO-RS analysis shows that the hydrogen bonding between the $[NTf_2]^-$ anion and water significantly contributes to the high endothermicity of the system. The endothermicity indicates that the hydrogen bonding between $[NTf_2]$ and water is much weaker than that between water molecules. On the opposite, spontaneous dissolution is observed for the $[C_4C_1im][Ac]$−water system, presenting γ_w^∞ lower than unity. The strong hydrogen bonding between $[Ac]^-$ anions and water leads to the exothermicity of the mixture, and eventually, the spontaneous dissolution of water in the IL. Furthermore, it has been shown that the binary mixtures composed of water and $[C_4C_1im][Ac]$ are miscible within the whole composition range.[21] Yet again, hydrogen bonding between water and the $[Ac]^-$ anion is responsible for their high miscibility.[21] Alternately, the $[C_4C_1im][NTf_2]$−water systems eventually lead to the appearance of liquid−liquid immiscibility.[27] Therefore, the temperature-dependency of the activity coefficient of water at infinite dilution in an IL, along with the estimated excess properties and COSMO-RS, can be used as a guideline regarding the miscibility of the ILs−water system, so that it eventually will have an impact on designing ILs with enhanced water absorption capacity.

On the basis of the results described above, besides the activity coefficient at infinite dilution assessment to discuss and interpret water−IL intermolecular interaction, we further evaluated the approach here proposed using the water partial molar excess enthalpy, entropy, and Gibbs free energy estimated from both experiment and the COSMO-RS model. In this work, a critical evaluation of the experimental data was carried out by comparing similar systems, and the symbols and the lines in the figures represent the experimental data and the COSMO-RS prediction calculations, respectively.

3.2.2. Effect of Ionic Liquids Anion. The influence of the anion on the γ_w^∞ in an IL can be assessed by examination of the experimental data diagrams and COSMO-RS predictions as presented in Figures 4 and 5 (and Figures 1S to 9S in the Supporting Information). With the cation headgroup and the alkyl chain length fixed, the experimental data available allows a direct comparison of the effect of several anions on the γ_w^∞ in $[C_4C_1im]$-based and $[C_4C_1pyrr]$-based ILs. As can be observed in Figure 4, for $[C_4C_1im]$-based ILs, the γ_w^∞ in $[C_4C_1im][NTf_2]$ is higher than unity; this is due to unfavorable interactions between the $[NTf_2]^-$ anion and water, as previously described. The opposite happens in all other studied $[C_4C_1im]$-based ILs, reflecting negative deviations to the ideality with the following sequence of increasing interactions with water: $[C_4C_1im]$-$[CF_3SO_3]$ < $[C_4C_1im][SCN]$ < $[C_4C_1im][TOS]$ < $[C_4C_1im]$-$[TFA]$ < $[C_4C_1im][MeSO3]$ ≈ $[C_4C_1im]Br$ < $[C_4C_1im]Cl$ < $[C_4C_1im][DMP]$ < $[C_4C_1im][Ac]$.

COSMO-RS is able to describe the positive deviation of $[C_4C_1im][NTf_2]$−water and negative deviation for all other studied systems as well as the temperature dependence. However, COSMO-RS could not correctly predict the position of $[C_4C_1im]Br$ according to the sequence given above.

dx.doi.org/10.1021/ie5021415 | Ind. Eng. Chem. Res. 2014, 53, 12466−12475

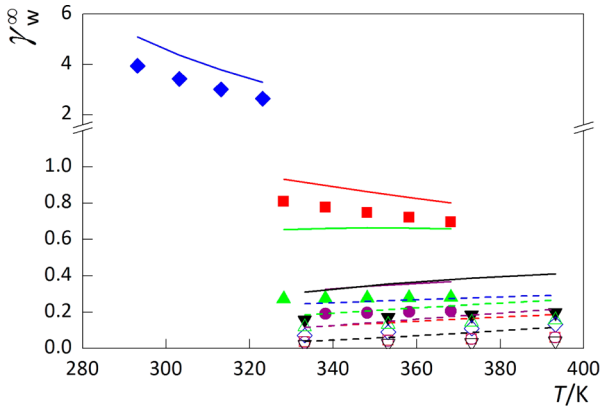

Figure 4. Water activity coefficient at infinite dilutionas a function of temperature for C_4C_1im cation based ILs. Symbols: (blue filled diamond, solid line), $[C_4C_1im][NTf_2]$;[39] (red filled square, solid line), $[C_4C_1im][CF_3SO_3]$;[41] (green filled triangle, solid line), $[C_4C_1im][SCN]$;[40] (purple filled circle, solid line), $[C_4C_1im][TOS]$;[21] (black filled triangle, solid line), $[C_4C_1im][TFA]$;[21] (black open diamond, dashed line), $[C_4C_1im]Br$;[21] (red open square, dashed line), $[C_4C_1im]Cl$;[21] (green open triangle, dashed line), $[C_4C_1im][MeSO_3]$;[21] (purple open circle, dashed line), $[C_4C_1im][DMP]$;[21] and (black open triangle, dashed line), $[C_4C_1im][Ac]$.[21]

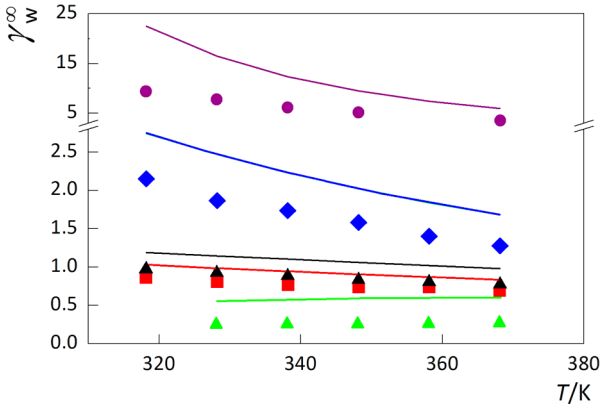

Figure 5. Water activity coefficient at infinite dilution as a function of temperature for C_4C_1pyrr cation based ILs. Symbols: (red square, line), $[C_4C_1pyrr][CF_3SO_3]$;[42] (green triangle, line), $[C_4C_1pyrr][SCN]$;[43] (blue diamond, line),$[C_4C_1pyrr][B(CN)_4]$;[44] (purple circle, line),$[C_4C_1pyrr][eFAP]$;[45] and (black triangle, line), $[C_4C_1pyrr][C(CN)_3]$.[46]

Nevertheless, it should be highlighted that the experimental data of γ_w^∞ in Br-containing ILs is very limited,[21] making it difficult to decide whether this peculiarity is either due to a failure of COSMO-RS or indicative of an irregular and unexpected behavior. More experimental data on γ_w^∞ in Br-containing ILs is required to start to understand the phenomena behind this particular observation.

Moving to Figure 5, the γ_w^∞ in $[C_4C_1pyrr]$-based ILs varies from 0.26 to 9.36 for $[C_4C_1pyrr][SCN]$ and $[C_4C_1pyrr]$-[eFAP], respectively. Like the γ_w^∞ in $[C_4C_1im][NTf_2]$, positive deviations to ideality are observed for the systems containing $[C_4C_1pyrr][eFAP]$ and $[C_4C_1pyrr][B(CN)_4]$, with the former presenting values significantly higher than unity. Favorable interactions are observed for the system containing $[C_4C_1pyrr]$ $[C(CN)_3]$, followed by $[C_4C_1pyrr][CF_3SO_3]^-$, and at last $[C_4C_1pyrr][SCN]$. Even though COSMO-RS overestimates the activity coefficient of water at infinite dilution, particularly in the highly hydrophobic ILs, as mentioned earlier, the temperature-dependence and the anion natures are well described by COSMO-RS for the $[C_4C_1pyrr]$-based ILs.

When the results depicted in Figures 4 and 5 (and Supporting Information, Figures 1S to 9S) are combined, it is striking to observe that the ILs that share the same anion present similar values of γ_w^∞, regardless the cation headgroup and alkyl chain length. For example, the γ_w^∞ in $[C_2C_1im][SCN]$, $[C_4C_1im][SCN]$, $[C_4\text{-}4\text{-}C_1py][SCN]$, $[C_4C_1pyrr][SCN]$, and $[C_4C_1pip][SCN]$ at 328.15 K are 0.27, 0.27, 0.31, 0.26, and 0.33, respectively. Thus, it seems clear that γ_w^∞ is more influenced by the ILs anion with only a small contribution from the headgroup and alkyl chain length, as will be discussed later. Therefore, for the $[C_4C_1\text{-}X]$-based ILs (with X = imidazolium, pyridinium, pyrrolidinium, or piperidinium), the anions can be ranked on the basis of increasing interaction with water as follows: $[eFAP]^- < [NTf_2]^- < [B(CN)_4]^- < [C(CN)_3]^- < [CF_3SO_3]^- < [SCN]^- \approx [N(CN)_2]^- < [TOS]^- < [TFA]^- < Br^- \approx [MeSO_3]^- < Cl^- < [DMP]^- < [Ac]^-$. The trend obtained here is also observed when these anions are coupled with different alkyl chain length and headgroup. Even for the series of ILs that incorporate functional groups such as hydroxyl and alkoxy (cf. Figures 5S and 7S-9S in the Supporting Information, respectively), the same trend of anions and temperature-dependence is also observed.

The partial molar excess properties can be used to further delve into the mechanism behind the dissolution of water in IL. Figure 6 displays the relationship between γ_w^∞ and the water

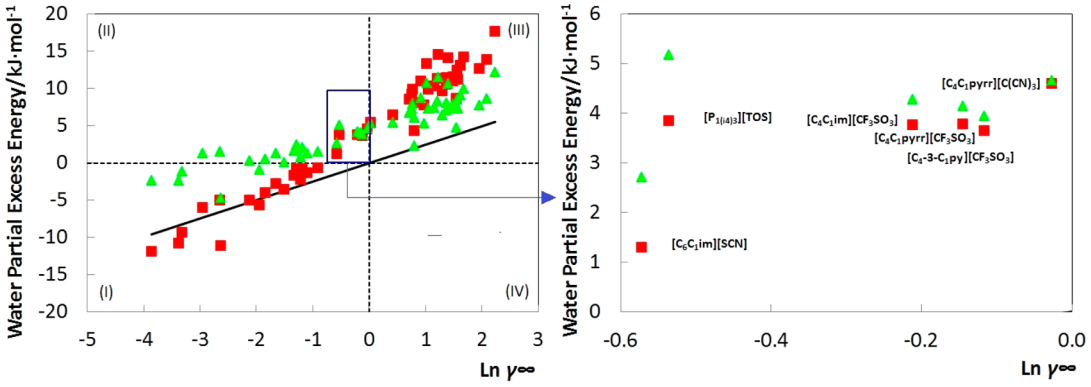

Figure 6. Relationship between the activity coefficient, γ_w^∞, and the water partial molar excess energy of water at infinite dilution in ILs at T_{ref} = 298.15 K estimated from experimental data. The line, (—) represents $\overline{G}_m^{E,\infty}$ and the symbols represent (red square) $\overline{H}_m^{E,\infty}$ and (green triangle) $T_{ref}\overline{S}_m^{E,\infty}$.

dx.doi.org/10.1021/ie5021415 | Ind. Eng. Chem. Res. 2014, 53, 12466−12475

partial molar excess properties calculated using the experimental data. Three different areas can be distinguished on the basis of this relationship. The region (I), corresponds to the ILs−water systems with negative deviations from Raoult's law, $\gamma_w^\infty < 1$ that is related to a spontaneous dissolution of water in the IL. Most ILs−water systems lie in this region composed by anions with strong hydrogen basicity, such as $[Ac]^-$. COSMO-RS reveals that for the water−$[C_4C_1im][Ac]$ system, the hydrogen bonding between water and $[Ac]^-$ anion is much stronger than hydrogen bonding between water molecules, and it eventually leads to an exothermic mixing behavior of this system. Thus, for the ILs located in this region, the exothermic mixing behavior of the $\bar{H}_m^{E,\infty}$ is occurs because anion−water interaction is greater than water−water or IL−IL cohesive energy. Indeed, it can observed that the lower is the water activity coefficients at infinite dilution in the IL, the more negative is the exothermicity of the solute in the solvent, relating to more favorable intermolecular interactions between water and IL with respect to pure compounds. This finding is in agreement with results reported by Iedema.[12]

It is, nevertheless, interesting to observe that some exceptions are observed, as depicted in Figure 6, in region (II), where $\gamma_w^\infty < 1$ and $\bar{G}_m^{E,\infty} <$ is negative, yet $\bar{H}_m^{E,\infty}$ is positive. It is observed that $[P_{1(i4)3}][TOS]$, $[C_6C_1im][SCN]$, $[C_4C_1pyrr][C(CN)_3]$, and several $[CF_3SO_3]$-based ILs, namely $[C_4C_1im][CF_3SO_3]$, $[C_4C_1pyrr][CF_3SO_3]$, and $[C_4\text{-}3\text{-}C_1py]$-$[CF_3SO_3]$, fall in region (II). Here we may have very special solutions for which $\bar{G}_m^{E,\infty}$ is close to 0, but for which $\bar{H}_m^{E,\infty}$ and $T_{ref}\bar{S}_m^{E,\infty}$ are both positive. It means that the enthalpic and entropic contributions cancel each other. Such solutions are obviously not ideal but they obey Raoult's law. Furthermore, for those ILs, except $[P_{1(i4)3}][TOS]$, COSMO-RS indicates that the hydrogen bonding of anion−water is energetically weak and does not overcome the loss of water−water hydrogen bonding upon mixing. Thus, to regain the lost hydrogen bonding network, the water molecules tend to use the energy of the system to reorient themselves. The lower is the entropy change, the easier is the reorientation taking place. Therefore, it also leads to spontaneous solvation of water in these ILs. Alternately, the temperature dependence of γ_w^∞ in $[P_{1(i4)3}]$-$[TOS]$[31] is quite interesting; the system presents negative deviation from ideality, yet the γ_w^∞ decreased (the interaction becomes more favorable) with increasing temperature.

For those water−IL systems setting along the region (III), where $\gamma_w^\infty > 1$ and naturally $\bar{G}_m^{E,\infty} > 0$ kJ·mol^{-1}, no particular affinity between IL and water molecules is observed. The ILs with a highly hydrophobic anion, such as $[eFAP]^-$ and $[NTf_2]^-$ fall within this criterion. Yet again, the hydrogen bonding between anion−water is still the dominant interaction, however not in the favorable way. The highly unfavorable interaction between water and anion in this region, eventually leads to the formation of immiscible solutions. That is, phase separation will be observed by mixing water and these ILs. Therefore, they may find themselves as potential solvents in liquid−liquid extraction from aqueous solution.[32,33]

On the basis of COSMO-RS, the water partial molar excess enthalpy can be further analyzed by the specific interactions arising from the individual ions. It reveals that the hydrogen bonding between anion and water is the major contribution to the total partial molar excess enthalpy of the system. That is, the more negative the contribution of hydrogen bonding of anion and water to the total partial molar excess enthalpy, the higher the interaction of ILs and water, as displayed by their lower γ_w^∞. Accordingly, the ranking of the anion interaction with water based on the partial molar excess enthalpies is the same as that reported above based on the γ_w^∞ and thus on the water partial molar excess Gibbs energy. This trend is also identical to that obtained from the solvatochromic parameter β, measuring the hydrogen-bond acceptor ability of the ILs,[34,35] and with the extended scale for the hydrogen-bond basicity of ILs recently proposed.[36] Thus, as previously observed for the excess enthalpy of the ILs−water mixtures,[26] the γ_w^∞ in ILs is dominated by the hydrogen-bond basicity of the anion.

In summary, it can be concluded that the hydrogen bonding between water and the IL anion plays a significant role on the interaction of the ILs with water. It considerably determines the enthalpic behavior of the binary mixtures composed by ILs and water. Those ILs with strong basicity display a high attraction toward water molecules, regardless of the type of cation headgroup. Nevertheless, as will be shown below, the cation headgroup and alkyl chain length, and the incorporation of a functional group also have some influence and, to a lesser extent, can be used further to fine-tune the affinity of ILs toward water molecules.

3.2.3. Effect of Cation Headgroup of the Ionic Liquids . The impact of the cation headgroup of the ILs on the γ_w^∞ can be evaluated by examination of the experimental $\gamma_w^\infty - T$ diagrams and their prediction using COSMO-RS as presented in Figures 7 and 8 (see also Figures 10S and 12S in the Supporting

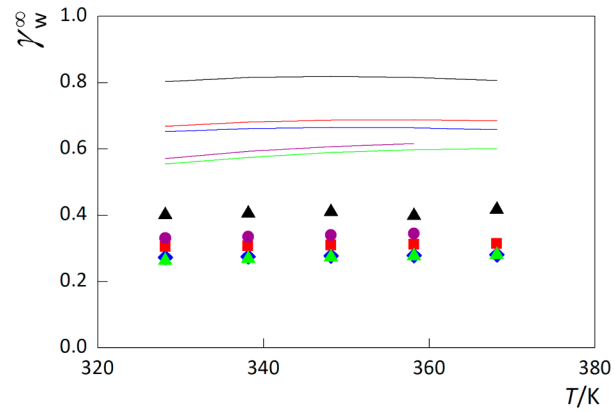

Figure 7. Water activity coefficient at infinite dilution as a function of temperature for the $[SCN]^-$ anion-based ILs. Symbols: (blue diamond, line), $[C_4C_1im][SCN]$;[40] (red square, line), $[C_4\text{-}4\text{-}C_1py]$-$[SCN]$;[43] (green triangle, line), $[C_4C_1pyrr][SCN]$;[43] (purple circle, line), $[C_4C_1pip][SCN]$;[47] and (black triangle, line), $[C_6iQui][SCN]$.[48]

Information). These two figures contain a series of ILs with two anions of different hydrogen-bond basicity. In Figure 7, the $[SCN]^-$ anion is retained for all studied cation headgroups, allowing the study of the impact of the cation headgroups on their interaction with water. It can be observed that all systems display a similar temperature dependence of γ_w^∞ further supporting the idea that the anion plays a major role, while the cation headgroup has a lower influence on their interaction with water. To get a wider picture on the effect of the cation headgroup, the water−$[C_6\text{-}iQui][SCN]$ complex is also considered in Figure 7, taking into account its small contribution to the γ_w^∞. Herein, it can be observed that the γ_w^∞ is the lowest for $[C_4C_1pyrr][SCN]$ indicating its highest interaction with water. It is followed by $[C_4C_1im][SCN]$, $[C_4\text{-}4\text{-}C_1py][SCN]$, $[C_4C_1pip][SCN]$, and at last, $[C_6\text{-}iQui][SCN]$. Despite COSMO-RS not being able to predict the strength of

dx.doi.org/10.1021/ie5021415 | Ind. Eng. Chem. Res. 2014, 53, 12466−12475

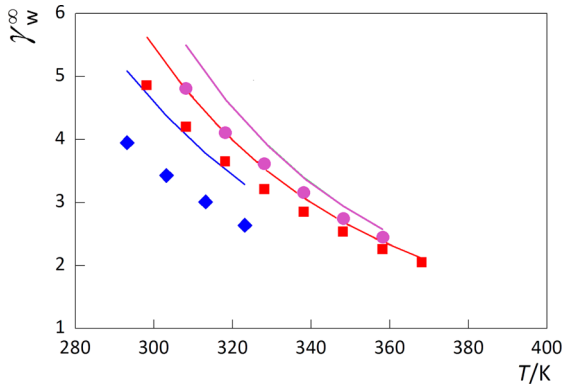

Figure 8. Water activity coefficient at infinite dilution as a function of temperature for $[NTf_2]^-$ anion-based ILs. Symbols: (blue diamond, line), $[C_4C_1im][NTf_2]$;[39] (red square, line),$[C_4\text{-}4\text{-}C_1py][NTf_2]$;[49] (purple circle), $[C_4C_1pip][NTf_2]$.[50]

water in $[C_4C_1pip][SCN]$, the general trend of the cation headgroup and temperature dependence of γ_w^∞ in these ILs is well predicted.

Since all the studied ILs displayed in Figure 7 share the same anion, [SCN], the differences of their γ_w^∞ can be attributed to the contribution of their cation head groups. The trend observed here is that the γ_w^∞ increases, that is, becomes more unfavorable, from imidazolium to pyridinium, and at last quinolinium, whereas, for the nonaromatic ring, the trend with increasing γ_w^∞ is observed from pyrrolidinium to piperidinium. Explicitly, the γ_w^∞ increases with increasing number of carbon atoms. In other words, it increases with increasing hydrophobicity of the cation headgroup. As previously mentioned, the water molecule presents a decreasing attraction toward the nonpolar group (cf. Figure 1). Therefore, the interaction of ILs with water can be increased with a reduction of the hydrophobicity of the cation headgroup. The trend of cation hydrophobicity can also be observed for the other studied ILs, as depicted in Figure 7 (and Figures 10S-12S in the Supporting Information).

In addition to the cation headgroup hydrophobicity, expressed in the previous paragraph, another factor, the cation−anion interaction strength, must also be taken into account for designing ILs with high water−IL interactions. In a previous work, we have performed the analysis of excess enthalpy for the binary mixture composed of water and ILs, and their modeling using COSMO-RS.[26] It was found that the hydrogen bonding strength of cation−water and anion−water determines the enthalpic nature of the systems. Furthermore, the ability of the IL anion to hydrogen bond with the water molecules is also dependent on the hydrogen bonding strength of cation−anion. This cation−anion interaction strength can be accessed by varying the cation headgroup combined with the same anion, as depicted in Figures 7 and 8 for $[SCN]^-$ or $[NTf_2]^-$, respectively. For the $[SCN]^-$containing ILs, the water partial molar excess enthalpies indicate that hydrogen bonding between $[SCN]^-$ water is thermodynamically stronger than water−water molecules, thus the establishment of new hydrogen bonding between the anion and water depends on the strength of the cation and anion interaction. As example, for the five-member ring of the cation headgroup, water presents a higher affinity toward $[C_4C_1pyrr][SCN]$ than $[C_4C_1im][SCN]$. It is well-known that the acidic protons of the imidazolium ring is capable of forming a hydrogen bond with its anion counterpart, in this case $[SCN]^-$, meanwhile the pyrrolidinium does not present this feature. On the basis of COSMO-RS model, the hydrogen bonding interaction in $[C_4C_1im][SCN]$ (-16.639 kJ·mol^{-1}) is higher than in $[C_4C_1pyrr][SCN]$ (-9.065 kJ·mol^{-1}). The strong hydrogen bonding between $[C_4C_1im]^+$ and $[SCN]^-$ restricts the interaction with the water molecules, and, consequently, it has less affinity toward water molecules when compared to $[C_4C_1pyrr][SCN]$.

The impact of cation−anion interaction strength toward water solvation in ILs is quite different when the hydrogen bonding between anion and water is weaker than that between water and water, as in the case for the series of $[NTf_2]$-based ILs. In Figure 8 it is observed that water has a higher affinity toward $[C_4C_1im][NTf_2]$, followed by $[C_4\text{-}4\text{-}C_1py][NTf_2]$, and at last $[C_4C_1pip][NTf_2]$. This trend is well predicted by COSMO-RS. The higher affinity of water toward $[C_4C_1im]$-$[NTf_2]$ and $[C_4\text{-}4\text{-}C_1py][NTf_2]$ can be also be addressed in terms of hydrophobicity, in which the former presents a lesser hydrophobic character than the latter. The positive enthalpy of the systems indicates that the hydrogen bonding between $[NTf_2]$ and water is weaker than that between water molecules. The only favorable interaction observed from COSMO-RS occurs between the cation and water. The higher affinity of aromatic ILs, $[C_4C_1im][NTf_2]$ and $[C_4\text{-}4\text{-}C_1py][NTf_2]$, toward the nonaromatic ILs$[C_4C_1pip][NTf_2]$ seems to be due to the interaction of the water with the π systems of those two ILs, while no electrons are available for privileged interaction on piperidinium. This is the opposite of what has been observed for the [SCN]-containing anion. Here, the cation headgroup actually "helps" contribute to its interaction with water and is not an obstacle as previously discussed for the [SCN]-containing ILs. This is connected to the fact that generally the magnitude of the cation headgroup effect is more evident when the anion has lower attraction to water.

In addition, it should be pointed out that the COSMO-RS prediction for γ_w^∞ in $[P_{1(i4)3}][TOS]$ presents much larger deviations to the experimental data, as depicted in Figure 10S of the Supporting Information. Interestingly, the $\gamma_w^\infty-T$ presents decrement on the γ_w^∞ with increasing temperature, even if it possesses γ_w^∞ lower than unity. This distinctive behavior may be addressed as either simply experimental error or a different mechanism of water solvation in branching structures that cannot be captured by COSMO-RS. It is known that COSMO-RS fails to correctly predict the mixture behavior whenever branched alkyl chains are present;[26,37] for example, it fails to describe excess enthalpy of binary mixtures composed by cholinium lactate and water,[28] and vapor liquid equilibria containing ILs and 2-propanol.[79] This result shows that while in general it can provide an adequate estimation of the experimental values of γ_w^∞ there is still room for improvement concerning the reliability of COSMO-RS.

3.2.4. Effect of the Cation Alkyl Chain Length. Figure 9 (and Figures 13S−16S in the Supporting Information) present the effect of the cation alkyl chain length on the γ_w^∞. As observed, an increase in alkyl chain leads to an increase in γ_w^∞, indicating less favorable interactions between water and the ILs, regardless the cation headgroup and anion nature. This behavior can be explained due to an increase in the hydrophobicity of the IL as depicted in Figures 17S and 18S, increasing alkyl chain increase the peak in the nonpolar region that lead to increment of the hydrophobic character. As a consequence, the ILs with a longer alkyl chain present lower affinity toward water molecules. The impact of temperature is

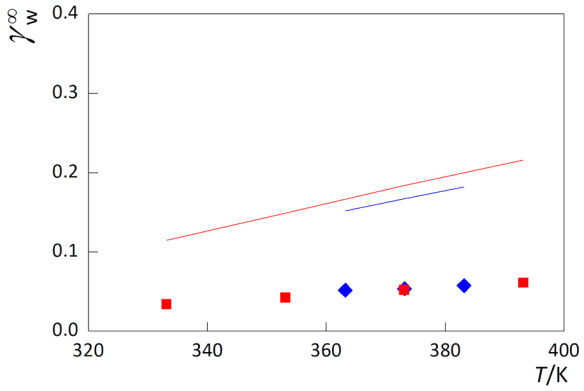

Figure 9. Water activity coefficient at infinite dilution as a function of temperature for $[DMP]^-$ anion-based ILs. Symbols: (blue diamond, line), $[C_1C1im][DMP]$;[51] (red square, line), $[C_4C_1im][DMP]$.[21]

highly dependent on the anion nature of the ILs as discussed previously, corroborating the idea that the anion controls their interaction with water. COSMO-RS is able to predict the alkyl chain length and temperature dependency observed experimentally. However, it should be highlighted that although the γ_w^∞ increases with the alkyl chain, the increment is rather small, particularly for the ILs with high hydrogen bonding basicity anions, such as $[DMP]^-$ depicted in Figure 9.

3.2.5. Effect of the Cation Functional Group. The effect of cooperating functional groups into the cation chain is displayed in Figure 9. Here, one of the carbons in $[C_4C_1pip][NTf2]$ and $[C_4C_1pyrr][eFAP]$ is substituted by an oxygen atom, providing them with an ether functional group, as in the case of $[COC_2C_1pip][NTf2]$ and $[COC_2C_1pyrr][eFAP]$, respectively. It is observed that the γ_w^∞ decreases by substituting the carbon atom with oxygen for both $[C_4C_1pip][NTf_2]$ and $[C_4C_1pyrr]$-$[eFAP]$. The trend is well described by COSMO-RS, despite the overestimation. Nevertheless, the substitution with a polar functional group does not change the temperature dependence of γ_w^∞.

The impact of incorporating polar groups into the cations of ILs having high basicity anion γ_w^∞ could not be found in the literature. Nevertheless, by using the experimental excess enthalpy and CHelpG Atomic Charge, it is suggested that the introduction of a polar group, namely a hydroxyl cluster on this type of cation, does not increase its hydrogen bonding with water, as shown by Ficke and Brennecke.[38] This can be understood from the preferential association of the anion with the hydroxyl group of the cation, decreasing the anion−water interaction.

3.3. Impact of Cation−Anion Interaction Strength toward IL Interaction with Water Molecule. The knowledge of intermolecular forces is a requisite for understanding IL properties and their affinity toward other molecules, such as water. It determines whether IL anions or ion pairs stick together or interact with water molecules at a given circumstance and is also dependent on the cation and anion. In this section, we discuss the importance of the cation−anion interactions in ILs and their relevance for the properties of these unique fluid materials. Using the COSMO-RS model the interaction energies in the IL, as well as their binary mixture with water, can be split into electrostatic-misfit, hydrogen bonding, and van der Waals forces. In a previous work, using COSMO-RS to predict the excess enthalpies of (IL + water) binary mixtures,[26] we have shown that the interaction strength between the anion and water determines the enthalpy of the system. In this way, the higher is the anion basicity, the stronger is its interaction with water molecules leading to an exothermic mixing behavior. However, the experimental data of excess enthalpy is limited to miscible systems. A broader picture of the anion impact on the interaction of the ILs with water can be drawn from the water activity coefficients at infinite dilution in ILs, as presented in this work. The data ranges from the most hydrophilic $[Ac]^-$ to the extremely hydrophobic $[eFAP]^-$ with a wide variety of cations as well. Excess enthalpy of (IL + water) and water activity coefficients at infinite dilution in IL, as well as the respective COSMO-RS modeling, converge into the notion that the anion plays a crucial role on IL interactions with water molecules.

Furthermore, the water activity coefficient at infinite dilution in an IL allows us to evaluate the impact of the IL cation, which also depends on the anion. In the first group, for the IL with low basicity anions, such as $[NTf_2]$, the cation plays its role as an interaction point with a water molecule. In the second group, for the IL with high basicity anions, the water activity coefficient highly depends on the cation−anion interaction. In terms of the interaction between an IL with high basicity anions and a water molecule, the cation−anion interaction strength can be summarized in the following rule of thumb: For the same anion, the stronger is the cation−anion interaction of a given IL, the weaker is the interaction between IL and water. As mentioned before, the interaction between IL and water is controlled by the anion basicity. To establish new hydrogen bonding between the anion−water molecules, the system must go through a breaking of hydrogen bonding between water molecules and also between the cation and anion. The change of the Gibbs free energy of the system upon mixing is a difference between the final state where the ions (or ion pairs) are interacting with the water molecules and the initial state with pure compounds interacting between them. In this way, if the cation bonds strongly to the anion, it requires a higher energy to break this bond to establish a new hydrogen bond with a water molecule thus decreasing the change of the Gibbs free energy of the system upon mixing, making it less favorable. For example, as depicted in Figure 7, the strong hydrogen bonding between $[C_4C_1im]^+$ and $[SCN]^-$ (-16.639 kJ·mol^{-1}) gives a higher restriction to the interaction with the water molecules when compared to the bonding of $[C_4C_1pyrr]$ and $[SCN]$ (-9.065 kJ·mol^{-1}).

This cation−anion interaction strength can definitely be used as a key factor, besides increasing anion basicity, to design an IL with enhanced affinity toward a water molecule. In this way, the target IL can be designed by combining a high basicity anion with a cation so as to have the weakest cation−anion interaction strength.[29]

4. CONCLUSION

ILs have been extensively studied as promising high performance liquids. With the very large number of possible cations and anions that can be used to form the ILs, finding the best ILs for a given application is not an easy task. Since it is not feasible to experimentally determine all the possible combinations of ILs, a predictive method capable of describing the phase behavior of such systems is of extreme importance. In this work, we have shown that COSMO-RS and its implementation in the program COSMOtherm is capable of giving satisfactory a priori predictions of γ_w^∞ in ILs, with a global average relative deviation of 27.2%, which may be of value for designing suitable ILs with

enhanced affinity toward water molecules. In all cases, the basicity of the ILs anion determines the behavior of the IL−water system, with headgroup and its alkyl chain having a minor impact that may be used to fine-tune the interactions. Although some larger deviations were also identified (that can be a motivation for COSMO-RS model improvement toward a better prediction capability) the COSMO-RS method proved to be a useful tool for explaining the impact of ILs structural variations on their interaction with water so as to screen potential ILs with improved water interactions.

■ ASSOCIATED CONTENT

Supporting Information

Supplementary figures and tables as described in the text. This material is available free of charge via the Internet at http://pubs.acs.org.

■ AUTHOR INFORMATION

Corresponding Author

*Tel: +351-234-370200. Fax: +351-234-370084. E-mail: jcoutinho@ua.pt.

Notes

The authors declare no competing financial interest.

■ ACKNOWLEDGMENTS

This work was financed by national funding from Fundação para a Ciência e a Tecnologia (FCT), through the projects PTDC/QUI-QUI/121520/2010, Pest-CTM/LA0011, and LSRE/LCM (project PEST-C/EQB/LA0020/2013). Kiki A. Kurnia acknowledges FCT for the postdoctoral grants SFRH/BPD/88101/2012.

■ REFERENCES

(1) Wasserscheid, P.; Welton, T. *Ionic Liquids in Synthesis*, 2nd ed.; Wiley-VCH Verlag GmbH & Co. KGaA: Darmstadt, Federal Republic of Germany, 2009; Vol. *1*.

(2) Walden, P. Molecular weights and electrical conductivity of several fused salts. *Bull. Russ. Acad. Sci.* **1914**, 405−422.

(3) Zhang, S. J.; Lu, X. M.; Zhou, Q.; Li, X.; Zhang, X.; Lu, S. *Ionic Liquids: Physicochemical Properties*, 1st ed.; Elsevier: Oxford, United Kingdom, 2009.

(4) Chen, Y.; Cao, Y.; Mu, T. A New Application of Acetate-Based Ionic Liquids: Potential Usage as Drying Materials. *Chem. Eng. Technol.* **2014**, *37*, 527−534.

(5) Wang, J.-F.; Li, C.-X.; Wang, Z.-H.; Li, Z.-J.; Jiang, Y.-B. Vapor pressure measurement for water, methanol, ethanol, and their binary mixtures in the presence of an ionic liquid 1-ethyl-3-methylimidazolium dimethylphosphate. *Fluid Phase Equilib.* **2007**, *255*, 186−192.

(6) Calvar, N.; González, B.; Gómez, E.; Domínguez, Á. Vapor−liquid equilibria for the ternary system ethanol + water + 1-butyl-3-methylimidazolium chloride and the corresponding binary systems at 101.3 kPa. *J. Chem. Eng. Data* **2006**, *51*, 2178−2181.

(7) Orchillés, A. V.; Miguel, P. J.; Llopis, F. J.; Vercher, E.; Martínez-Andreu, A. Isobaric vapor−liquid equilibria for the extractive distillation of ethanol + water mixtures using 1-ethyl-3-methylimidazolium dicyanamide. *J. Chem. Eng. Data* **2011**, *56*, 4875−4880.

(8) Khamooshi, M.; Parham, K.; Atikol, U. Overview of ionic liquids used as working fluids in absorption cycles. *Adv. Mech. Eng.* **2013**, *2013*, 7 Article ID 620592.

(9) Swarnkar, S. K.; Venkatarathnam, G.; Ayou, D. S.; Bruno, J. C.; Coronas, A. In *A Review on Absorption Heat Pumps and Chillers Using Ionic liquids as Absorbents*. International Workshop on Ionic Liquids−Seeds for New Engineering Applications, Lisbon, Portugal, 2−3 February 2012.

(10) Kim, Y. J.; Kim, S.; Joshi, Y. K.; Fedorov, A. G.; Kohl, P. A. In *Exergy Analysis of an Absorption Refrigeration System Using an Iconic Liquid as a Working Fluid in the Chemical Compressor*. International Refrigeration and Air Conditioning Conference, Purdue University, Purdue University, 2012.

(11) Seiler, M.; Kühn, A.; Ziegler, F.; Wang, X. Sustainable cooling strategies using new chemical system solutions. *Ind. Eng. Chem. Res.* **2013**, *52*, 16519−16546.

(12) Iedema, P. D. Mixtures for the absorption heat pump. *Int. J. Refrig.* **1982**, *5*, 262−273.

(13) Bhargava, B. L.; Yasaka, Y.; Klein, M. L. Computational studies of room temperature ionic liquid−water mixtures. *Chem. Commun.* **2011**, *47*, 6228−6241.

(14) Eike, D. M.; Brennecke, J. F.; Maginn, E. J. Predicting infinite-dilution activity coefficients of organic solutes in ionic liquids. *Ind. Eng. Chem. Res.* **2004**, *43*, 1039−1048.

(15) Tämm, K.; Burk, P. QSPR analysis for infinite dilution activity coefficients of organic compounds. *J. Mol. Model.* **2006**, *12*, 417−421.

(16) Ge, M.; Li, C.; Ma, J. QSPR analysis for infinite dilution activity coefficients of organic solutes in ionic liquids. *Electrochemistry* **2009**, *77*, 745−747.

(17) Diedenhofen, M.; Eckert, F.; Klamt, A. Prediction of infinite dilution activity coefficients of organic compounds in ionic liquids using COSMO-RS. *J. Chem. Eng. Data* **2003**, *48*, 475−479.

(18) Klamt, A. *COSMO-RS from Quantum Chemistry to Fluid Phase Thermodynamics and Drug Design*; Elsevier: Amsterdam, The Netherlands, 2005.

(19) Klamt, A.; Eckert, F. COSMO-RS: A novel and efficient method for the a priori prediction of thermophysical data of liquids. *Fluid Phase Equilib.* **2000**, *172*, 43−72.

(20) Banerjee, T.; Khanna, A. Infinite dilution activity coefficients for trihexyltetradecyl phosphonium ionic liquids: Measurements and COSMO-RS prediction. *J. Chem. Eng. Data* **2006**, *51*, 2170−2177.

(21) Khan, I.; Kurnia, K. A.; Mutelet, F.; Pinho, S. P.; Coutinho, J. A. P. Probing the interactions between ionic liquids and water: Experimental and quantum chemical approach. *J. Phys. Chem. B* **2014**, *118*, 1848−1860.

(22) *Turbomole*, version 6.1; University of Karlsruhe and Forschungszentrum Karlsruhe GmbH: Karlsruhe, Germany, 2009; http://www.turbomole.com.

(23) Eckert, F.; Klamt, A., *COSMOtherm*, version C3.0, release 13.01; COSMOlogic GmbH & Co. KG, Leverkusen, Germany, 2013.

(24) Diedenhofen, M.; Klamt, A. COSMO-RS as a tool for property prediction of IL mixtures—A review. *Fluid Phase Equilib.* **2010**, *294*, 31−38.

(25) Freire, M. G.; Ventura, S. P. M.; Santos, L. M. N. B. F.; Marrucho, I. M.; Coutinho, J. A. P. Evaluation of COSMO-RS for the prediction of LLE and VLE of water and ionic liquids binary systems. *Fluid Phase Equilib.* **2008**, *268*, 74−84.

(26) Kurnia, K. A.; Coutinho, J. A. P. Overview of the excess enthalpies of the binary mixtures composed of molecular solvents and ionic liquids and their modeling using COSMO-RS. *Ind. Eng. Chem. Res.* **2013**, *52*, 13862−13874.

(27) Freire, M. G.; Carvalho, P. J.; Gardas, R. L.; Marrucho, I. M.; Santos, L. M. N. B. F.; Coutinho, J. A. P. Mutual solubilities of water and the $[C_n mim][Tf_2N]$ hydrophobic ionic liquids. *J. Phys. Chem. B* **2008**, *112*, 1604−1610.

(28) Freire, M. G.; Neves, C. M. S. S.; Carvalho, P. J.; Gardas, R. L.; Fernandes, A. M.; Marrucho, I. M.; Santos, L. M. N. B. F.; Coutinho, J. A. P. Mutual solubilities of water and hydrophobic ionic liquids. *J. Phys. Chem. B* **2007**, *111*, 13082−13089.

(29) Kurnia, K. A.; Pinho, S. P.; Coutinho, J. A. P. Designing ionic liquids for absorptive cooling. *Green Chem.* **2014**, DOI: 10.1039/C4GC00954A.

(30) Freire, M. G.; Neves, C. M. S. S.; Shimizu, K.; Bernardes, C. E. S.; Marrucho, I. M.; Coutinho, J. A. P.; Canongia Lopes, J. N.; Rebelo, L. P. N. Mutual solubility of water and structural/positional isomers of *N*-alkylpyridinium-based ionic liquids. *J. Phys. Chem. B* **2010**, *114*, 15925−15934.

(31) Domanska, U.; Paduszynski, K. Gas−liquid chromatography measurements of activity coefficients at infinite dilution of various organic solutes and water in tri-iso-butylmethylphosphonium tosylate ionic liquid. *J. Chem. Thermodyn.* **2010**, *42*, 707−711.
(32) Chapeaux, A.; Simoni, L. D.; Ronan, T. S.; Stadtherr, M. A.; Brennecke, J. F. Extraction of alcohols from water with 1-hexyl-3-methylimidazolium bis(trifluoromethylsulfonyl)imide. *Green Chem.* **2008**, *10*, 1301−1306.
(33) Simoni, L. D.; Chapeaux, A.; Brennecke, J. F.; Stadtherr, M. A. Extraction of biofuels and biofeedstocks from aqueous solutions using ionic liquids. *Comput. Chem. Eng.* **2010**, *34*, 1406−1412.
(34) Jessop, P. G.; Jessop, D. A.; Fu, D.; Phan, L. Solvatochromic parameters for solvents of interest in green chemistry. *Green Chem.* **2012**, *14*, 1245−1259.
(35) Ab Rani, M. A.; Brant, A.; Crowhurst, L.; Dolan, A.; Lui, M.; Hassan, N. H.; Hallett, J. P.; Hunt, P. A.; Niedermeyer, H.; Perez-Arlandis, J. M.; Schrems, M.; Welton, T.; Wilding, R. Understanding the polarity of ionic liquids. *Phys. Chem. Chem. Phys.* **2011**, *13*, 16831−16840.
(36) Claudio, A. F. M.; Swift, L.; Hallett, J. P.; Welton, T.; Coutinho, J. A. P.; Freire, M. G. Extended scale for the hydrogen-bond basicity of ionic liquids. *Phys. Chem. Chem. Phys.* **2014**, *16*, 6593−6601.
(37) Freire, M. G.; Santos, L. M. N. B. F.; Marrucho, I. M.; Coutinho, J. A. P. Evaluation of COSMO-RS for the prediction of LLE and VLE of alcohols + ionic liquids. *Fluid Phase Equilib.* **2007**, *255*, 167−178.
(38) Ficke, L. E.; Brennecke, J. F. Interactions of ionic liquids and water. *J. Phys. Chem. B* **2010**, *114*, 10496−10501.
(39) Krummen, M.; Wasserscheid, P.; Gmehling, J. Measurement of activity coefficients at infinite dilution in ionic liquids using the dilutor technique. *J. Chem. Eng. Data* **2002**, *47*, 1411−1417.
(40) Domańska, U.; Laskowska, M. Measurements of activity coefficients at infinite dilution of aliphatic and aromatic hydrocarbons, alcohols, thiophene, tetrahydrofuran, MTBE, and water in ionic liquid [BMIM][SCN] using GLC. *J. Chem. Thermodyn.* **2009**, *41*, 645−650.
(41) Domańska, U.; Marciniak, A. Activity coefficients at infinite dilution measurements for organic solutes and water in the ionic liquid 1-butyl-3-methylimidazolium trifluoromethanesulfonate. *J. Phys. Chem. B* **2008**, *112*, 11100−11105.
(42) Domańska, U.; Redhi, G. G.; Marciniak, A. Activity coefficients at infinite dilution measurements for organic solutes and water in the ionic liquid 1-butyl-1-methylpyrrolidinium trifluoromethanesulfonate using GLC. *Fluid Phase Equilib.* **2009**, *278*, 97−102.
(43) Domańska, U.; Królikowska, M. Measurements of activity coefficients at infinite dilution in solvent mixtures with thiocyanate-based ionic liquids using GLC technique. *J. Phys. Chem. B* **2010**, *114*, 8460−8466.
(44) Domanska, U.; Królikowski, M.; Acree, W. E., Jr. Thermodynamics and activity coefficients at infinite dilution measurements for organic solutes and water in the ionic liquid 1-butyl-1-methylpyrrolidinium tetracyanoborate. *J. Chem. Thermodyn.* **2011**, *43*, 1810−1817.
(45) Domańska, U.; Lukoshko, E. V.; Królikowski, M. Measurements of activity coefficients at infinite dilution for organic solutes and water in the ionic liquid 1-butyl-1-methylpyrrolidinium tris(pentafluoroethyl)trifluorophosphate ([BMPYR][FAP]). *Chem. Eng. J.* **2012**, *183*, 261−270.
(46) Domańska, U.; Lukoshko, E. V. Measurements of activity coefficients at infinite dilution for organic solutes and water in the ionic liquid 1-butyl-1-methylpyrrolidinium tricyanomethanide. *J. Chem. Thermodyn.* **2013**, *66*, 144−150.
(47) Domańska, U.; Królikowski, M. Measurements of activity coefficients at infinite dilution for organic solutes and water in the ionic liquid 1-butyl-1-methylpiperidinium thiocyanate. *J. Chem. Eng. Data* **2011**, *56*, 124−129.
(48) Królikowska, M.; Karpińska, M.; Królikowski, M. Measurements of activity coefficients at infinite dilution for organic solutes and water in *N*-hexylisoquinolinium thiocyanate, [HiQuin][SCN] using GLC. *J. Chem. Thermodyn.* **2013**, *62*, 1−7.
(49) Domanska, U.; Marciniak, A. Activity coefficients at infinite dilution measurements for organic solutes and water in the ionic liquid 4-methyl-*N*-butyl-pyridinium bis(trifluoromethylsulfonyl)-imide. *J. Chem. Thermodyn.* **2009**, *41*, 1350−1355.
(50) Paduszyński, K.; Domańska, U. Limiting activity coefficients and gas-liquid partition coefficients of various solutes in piperidinium ionic liquids: Measurements and LSER calculations. *J. Phys. Chem. B* **2011**, *115*, 8207−8215.
(51) Kato, R.; Gmehling, J. Activity coefficients at infinite dilution of various solutes in the ionic liquids $[MMIM]^+[CH_3SO_4]^-$, $[MMIM]^+[CH_3OC_2H_4SO_4]^-$, $[MMIM]^+[(CH_3)_2PO_4]^-$, $[C_5H_5NC_2H_5]+[(CF_3SO_2)_2N]^-$ and $[C_5H_5NH]^+[C_2H_5OC_2H_4OSO_3]$. *Fluid Phase Equilib.* **2004**, *226*, 37−44.